Contact Angle Hysteresis and Sliding Angle of Commercial Hydrophobic Materials for Electrowetting Actuating Surface

M. Z. Yaacob, E. N. A. Latip[*]
School of Mechanical Engineering, College of Engineering,
Universiti Teknologi MARA, 40450 Shah Alam, Selangor, MALAYSIA
[*]*elinadia@uitm.edu.my*

ABSTRACT

Hydrophobic materials are one of the main components in electrowetting-on-dielectric (EWOD) devices, acting as the actuating surface upon which droplets move. EWOD technology has been extensively utilised as a platform for particle detection due to its versatility, simple design, and minimal waste. However, the technology could be more widely adopted if the materials and fabrication costs could be reduced. This study presents an investigation into two off-the-shelf hydrophobic materials as alternatives to conventional materials for the actuating surface component of the device. The surfaces were prepared using two different deposition methods, which were spin coating and spray coating. For each method, samples with two thicknesses were prepared, consisting of one layer and two layers. The contact angle hysteresis and sliding angle of the commercial hydrophobic surfaces were measured. One of the surfaces exhibited good performance with a contact angle hysteresis and sliding angles of 28° and 34°, respectively. These promising findings suggest the potential use of commercial hydrophobic materials for the future development of disposable and low-cost EWOD devices.

Keywords: *Hydrophobic Materials; Contact Angle Hysteresis; Sliding Angle; Electrowetting-On-Dielectric*

Introduction

Hydrophobic surfaces are materials that exhibit strong water-repellent behaviour, causing water droplets to bead up and roll off instead of spreading

ISSN 1823-5514, eISSN 2550-164X

https://doi.org/10.24191/jmeche.v13i1.2781
Received for review: 2024-06-14
Accepted for publication: 2024-10-10
Published: 2024-11-15

out and wetting the surface. The key principle underlying hydrophobicity is the minimisation of the contact area between water and the surface, which arises from two main factors, surface roughness, and low surface energy due to the presence of specific chemical compounds [1]-[2]. This unique response of the surface to water results in self-cleaning and anti-fouling properties, which are very useful in many applications, including industrial and aerospace coatings [3]-[5], medical devices [6], electronics [7], and, textiles [8], among others.

Electrowetting-on-dielectric (EWOD) is another technology that harness the distinctive property of hydrophobic materials to facilitate droplet motion [9]-[10]. In an EWOD-based device, a low-energy surface is desired as the actuating surface where liquid droplets are moved across the device using electrostatic energy. A basic set-up of the EWOD device consists of four main components: a substrate, an electrode or an array of electrodes, a dielectric layer, and a hydrophobic actuating surface, as shown in Figure 1. The contact angle of a liquid droplet sitting on the surface is regulated by the Young-Lippmann equation given as follows:

$$cos\,\theta_v = cos\,\theta_0 + \frac{\varepsilon_0 \varepsilon_r V^2}{2\gamma_{lg} d} \quad (1)$$

where θ_v is the apparent contact angle, θ_0 is the Young's contact angle, ε_0 is the relative permittivity, ε_r is the dielectric material's constant, V is the applied voltage, γ_{lg} is the liquid-gas interfacial energy, and d is the dielectric layer thickness.

When a voltage is applied across the droplet, electrostatic energy will be stored in the dielectric layer which will cause the droplet contact line to move forward. This will result in the spreading of the droplet and its contact angle, θ_v is reduced according to the Young-Lippmann equation. The detailed interpretation of the mechanism can be found in [11].

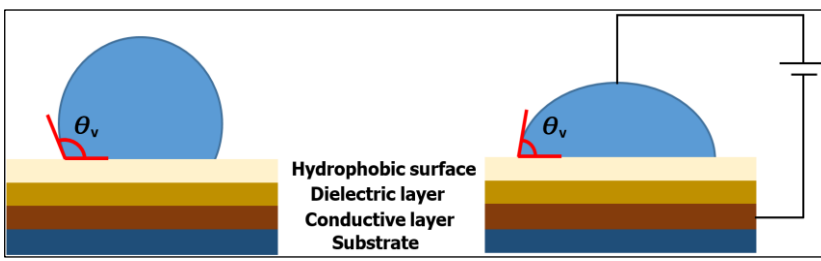

Figure 1: Basic set-up of an electrowetting-on-dielectric system (left), the droplet is activated when a voltage is applied across the droplet (right)

EWOD is widely used in lab-on-a-chip technology to perform specific functions such as Deoxyribonucleic Acid (DNA) assays (e.g., polymerase chain reaction) [12]-[14], cell-based assays (e.g., cell sorting and cell culture) [15]-[16], and immunoassays (e.g., rubella antibody detection) [17]. The self-cleaning property of the hydrophobic surface of EWOD devices has also been exploited to collect contaminants from surfaces exposed to specific environments using water droplets, to detect harmful particles [18]-[20]. The most commonly reported hydrophobic materials in EWOD are Teflon™ AF and Cytop®. They offer high initial contact angles of above 90° and high electrowetting reversibility which is the ability of droplet contact angle to return to its initial value after voltage application. Some devices utilise superhydrophobic materials with contact angles exceeding 150° as a strategy to reduce particle adhesion to the surface when liquid droplets laden with biomolecules or proteins are used [20]-[22].

EWOD stands out as one of the most popular mechanisms in lab-on-a-chip technology due to its high throughput and versatility in both architecture and application. An integrated EWOD platform, including the microcontroller, the detection system, and other auxiliary components, is compact and can be made portable [13], [23]-[24]. While many EWOD devices have been developed and proven successful in performing their intended functions, one obstacle to implementing them widely outside laboratory settings is their affordability [25]-[28]. The cost of an EWOD device can be quite expensive due to the high costs of materials and the fabrication process. Teflon™ AF and Cytop® are proprietary technologies and superhydrophobic surfaces often require specific processes and equipment for synthesis. To overcome this, some studies have utilised commercial hydrophobic products such as Rain-X [29]-[32], Nevosil Si-7100 [33], Avam [33] and superhydrophobic material such as NeverWet® [22], [34]. The findings of these studies have demonstrated the feasibility of using commercial coatings in the fabrication of EWOD devices, however, the surface properties—namely contact angle hysteresis and sliding angle—of any of these alternative materials have not been thoroughly investigated and reported yet. This paper aims to fill this gap by investigating the surface properties of commercial materials, which are crucial indicators of how effectively droplets can move across a surface.

To reduce high material costs, two commercially available hydrophobic materials are proposed for the investigation. One product, Renapur Protector, is approximately 12 times cheaper, while the other, Liquiproof LABS, is roughly 6 times less expensive than Cytop®. The hydrophobicity through contact angle measurement and the sliding angle and force required to instigate motion on these surfaces were examined. Different deposition methods were used in the preparation of the samples to explore which technique produces the best-performing surface.

Methodology

Hydrophobic sample preparation

Two types of commercial materials were employed: Liquiproof LABS Premium Protector (Liquiproof LABS, Wirral, UK) and Renapur Protector (Renapur Limited, Ashington, UK). Both materials are available in liquid form in a spray bottle and marketed as products for shoe protection from dirt and water. The substrate used for the sample was the standard microscope glass slides (Sail Brand, China).

Two deposition methods were used for both materials: spin coating, and spray coating. For each type of deposition method, two types of thickness were prepared: 1-layer and 2-layer samples. The spin coating (VT M-100, China) was performed at 2000 rpm for 60 s. All samples were cured on a hot plate at 100 °C for 15 minutes. For the two-layer samples, a second layer was applied after the curing process and the same deposition and curing steps were repeated.

Surface roughness

Surface roughness measurement was conducted using Surftest SV-600 (Mitutoyo America Corporation, Illinois, USA).

Contact angle measurements

Contact angle measurement was conducted using Water Surface Analysis System VCA 3000S (AST Products, Inc., Massachusetts, USA). A droplet of 5 μL was used for the static contact angle measurement. For the advancing and receding angles measurements, the protocol for the advancing and receding angles measurement was closely followed as suggested by Huhtamäki et al. [35], using the needle method. An initial 3 μL droplet was dispensed onto the sample's surface before the measurement was started. Droplet volume was then added gradually up to 10 μL. During this process, the droplet contact line was observed to measure the contact angle the moment the droplet contact line started to move outward. This contact angle was recorded as the Advancing Contact Angle (ACA). The receding contact angle (RCA) was measured by withdrawing the droplet volume gradually from 10 μL back to 3 μL. The contact angle reached RCA once the droplet contact line began to move inward and measurement of the contact was performed at that instance. Figure 2 shows the measurements of ACA and RCA of a water droplet on one of the hydrophobic samples [35]. The Contact Angle Hysteresis (CAH) measurement was repeated four times for each sample type.

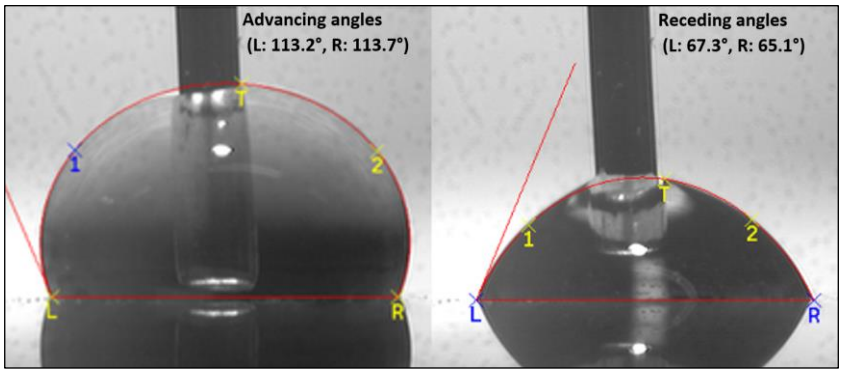

(a) (b)

Figure 2: Contact angle hysteresis measurement using needle method, (a) advancing angle and (b) receding angle

Sliding angle measurements

Sliding angle measurement was conducted to determine the required tilting angle to initiate the sliding down motion of a deionised (DI) water droplet from its resting position. Approximately half of the sample's substrate was positioned on top of a static platform while the other half was taped to a small laboratory jack. The substrate was ensured to be horizontally positioned on the platform and the laboratory jack surface using a bubble level before measurements were taken. Three droplet volumes were employed for the measurement: 5 μL, 10 μL, and 15 μL. The sample was tilted gradually by increasing the height of the laboratory jack slowly and stopped when the droplet started to slide down the surface. A laboratory protractor was used to measure the sliding angle of the substrate.

Results and Discussion

Surface roughness

Table 1 displays the surface roughness, *Ra*, of two commercial hydrophobic materials: Liquiproof and Renapur. There are four types of samples for each material, varying in deposition methods (i.e. spin coating, and spray coating) and the number of layers (1-layer and 2-layer). Overall, Renapur exhibits lower roughness compared to Liquiproof. Between the two deposition methods, spin coating produces the lowest roughness for both Liquiproof and Renapur materials. Spray-coated samples have the highest surface roughness for both materials, and the highest roughness for all types of samples is 2-layer spray-coated Liquiproof with 0.596 μm. In terms of the number of layers, the 2-layer samples exhibit higher roughness compared to the 1-layer samples.

Table 1: Surface roughness, Ra of the Liquiproof and Renapur hydrophobic materials for different deposition methods and number of layer.

Deposition method	Number of layers	Surface roughness, *Ra*, (μm)	
		Liquiproof	Renapur
Spin coating	1	0.007	0.008
	2	0.010	0.008
Spray coating	1	0.195	0.087
	2	0.596	0.110

In general, the deposition method significantly influenced the surface roughness of the samples, with spray coating yielding higher roughness compared to the spin coating method. Spin-coating produces a smoother surface due to the more uniform spreading of the hydrophobic material, as the automated spinning action distributes the material evenly across the substrate. In contrast, spray-coating ejects droplets of the material that spread upon impact with the substrate. The resulting layer is less even due to the varying sizes of the droplets and the manual operator's technique of pressing the spray button. The samples in this study produce surface roughness comparable to that of conventional hydrophobic materials, particularly the spin-coated samples. The reported roughness of Cytop® is 0.007 μm using the spin coating method [22].

Contact angle measurements

Static contact angle

One of the desirable properties for actuating surface in an EWOD device is a high initial contact angle indicating good hydrophobicity. Figure 3 shows the Young's contact angle of DI water sitting on the four different surfaces of the hydrophobic samples. All types of surfaces have a contact angle higher than 110° ranging between 114° - 118°. The 1-layer spray-coated Renapur has the highest contact angle with 118.4°. These values of contact angle are comparable to conventional hydrophobic materials such as Cytop® and Teflon™ AF which have contact angles of 110° - 117° [21].

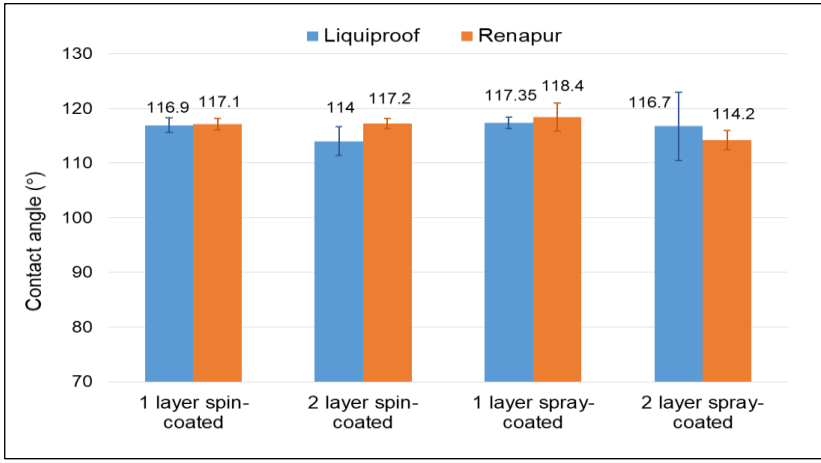

Figure 3: Static contact angle of the hydrophobic Liquiproof and Renapur hydrophobic materials varying in deposition methods and number of layers

Contact angle hysteresis

Contact angle hysteresis (CAH) is the difference between the advancing angle, θ_A and the receding angle, θ_R; i.e., $\theta_A - \theta_R$. The value can be a good indicator of the force or work required to move the contact line of a droplet sitting on a surface. Equation (2) represents the force required for contact line movement:

$$F = \gamma_{lg}(\cos\theta_R - \cos\theta_A) \quad (2)$$

where, γ_{lg} is the liquid-vapour surface tension. From Equation (2), the higher the hysteresis the higher the force needed to move the droplet contact line [36].

Figure 4 illustrates an example of one of the four hysteresis cycle runs for the 2-layer spin-coated Renapur and Liquiproof materials. As shown in the figure, during the advancing angle measurement, the initial contact angle increases slightly as the volume increases until it reaches θ_A and then stabilizes. When the volume decreases for the receding angle measurement, the contact angle decreases until it reaches θ_R and stabilizes again. Similar behaviour was observed across all surface types with varying CAH values.

Figure 5 summarises the average contact angle hysteresis for all types of surfaces. The best performing surface is a 2-layer spin-coated Renapur with the lowest recorded CAH at 27.5°. Generally, spin-coated surfaces have a lower CAH compared to spray-coated surfaces for both types of hydrophobic materials. The Ra values on spray-coated surfaces are higher compared to the spin-coated samples, implying that the CAH also increased as the surface became rougher. This observation aligns with the findings of Suzuki et al. [37], who studied the effect of roughness on the CAH of fluoroalkyl silane coatings.

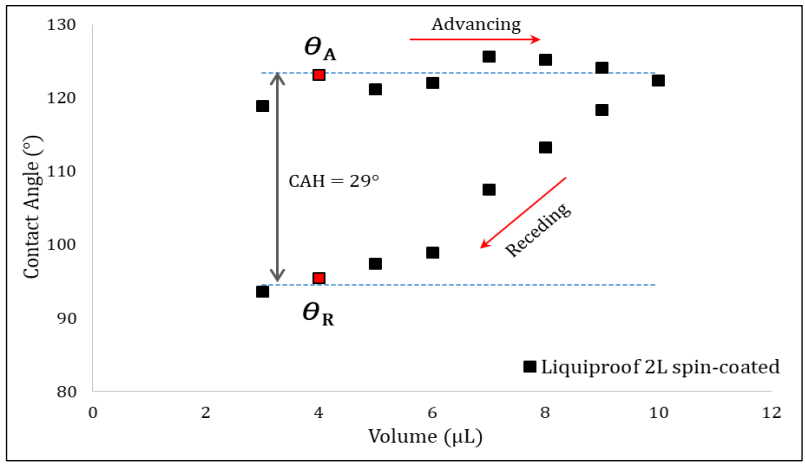

(a)

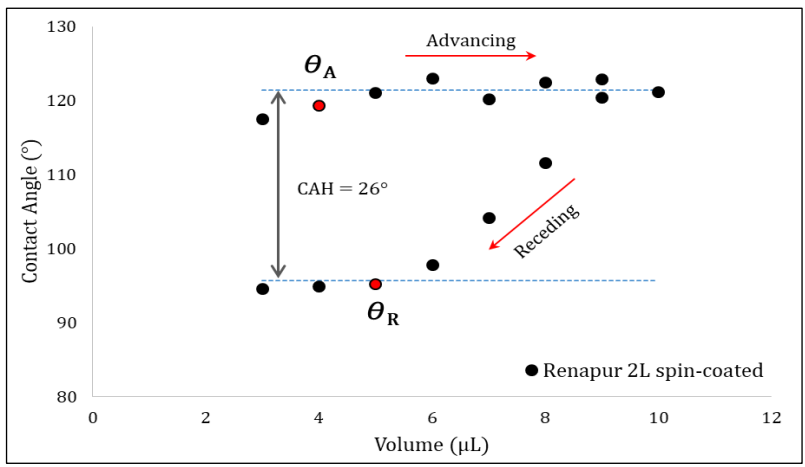

(b)

Figure 4: One of the four runs of hysteresis cycle for 2-layer spin-coated (a) Liquiproof and (b) Renapur materials. The red data points indicate the onset of the advancing (θ_A) and receding angles (θ_R), and the contact angle hysteresis (CAH) is the difference between the two angles.

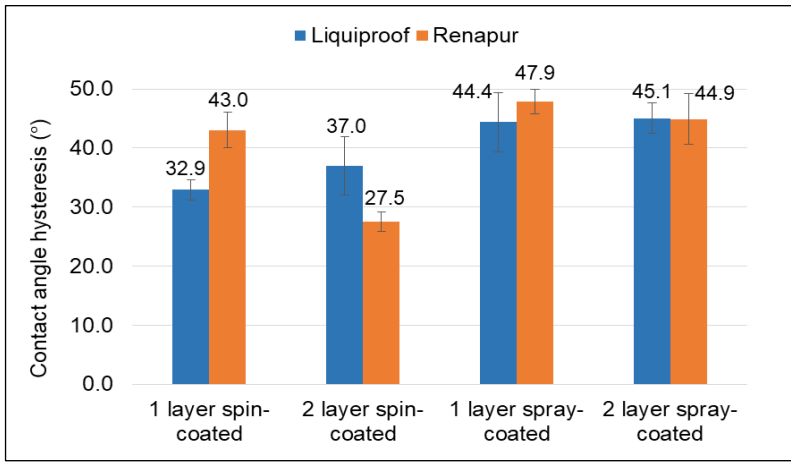

Figure 5: Contact angle hysteresis of the hydrophobic Liquiproof and Renapur hydrophobic materials varying in deposition methods and number of layers

Among samples of the same material and deposition method, the number of layers most significantly affects Renapur spin-coated samples. There is an approximate 36% reduction in CAH when a second layer is deposited on the surface. Chae et al. [21], reported similar findings, where CAH decreased with increasing layer thickness for both Teflon™ AF and Cytop® hydrophobic materials. While Renapur material follows the same trend as the previous study, for Liquiproof, the CAH increased with layer thickness albeit insignificantly.

Butt et al. [38] proposed that heterogeneity and surface roughness are the two main contributors to the CAH mechanism on solid surfaces. Molecular interaction also plays a role in CAH and Law [39] emphasized that CAH is primarily attributed to differences in liquid−solid interaction near the contact line during its movement. Although our study does not investigate the surface elemental composition of the hydrophobic materials, it has been established that chemical heterogeneity, as demonstrated by Suzuki et al. [37], can influence CAH. Moreover, small hydrophilic areas or patches of heterogeneous areas may exist on the hydrophobic surface, particularly for spray-coated samples during the deposition process, given the process's reliance on the manual operator's skills and consistency. Consequently, a future elemental surface analysis could provide a comprehensive understanding of the CAH behaviour of these surfaces.

Sliding angle measurements and force required for droplet movement

The sliding angle measurements for hydrophobic surfaces are presented in Table 2. The measurements were conducted using three droplet volumes: 5 µL, 10 µL, and 15 µL. All types of spin-coated samples demonstrated droplet sliding for 10 µL and 15 µL droplets when tilted. Two types of spray-coated samples, namely, 2-layer Liquiproof, and 1-layer Renapur, failed to exhibit any droplet movement after tilting the substrate up to 90° when 10 µL droplet was employed. For the 5 µL droplets, only two of the surfaces were capable of inducing droplet movement when tilted, specifically both of the spin-coated Renapur surfaces. Initiating movement for the 5 µL droplet is more challenging due to the relatively low volume, which makes it less susceptible to gravitational forces.

For a 15 µL droplet, the 2-layer spin-coated Renapur surface demonstrates the best performance, requiring the smallest sliding angle at 34°. Renapur material consistently outperforms Liquiproof, particularly in spin-coated samples, where it necessitates a lower sliding angle to initiate droplet sliding. The 2-layer spin-coated Renapur also requires less force compared to the 1-layer counterpart, which aligns with the CAH results for where this surface exhibits the lowest hysteresis.

Table 2: Sliding angle required to initiate droplet sliding on the Liquiproof and Renapur hydrophobic surfaces with varying deposition methods and number of layer

Hydrophobic material	Deposition method	Number of layers	Sliding angle, α (°)			Force, F (µN)		
			5µL	10µL	15µL	5µL	10µL	15µL
Liquiproof	Spin coating	1	-	60	42	-	84.8	98.3
		2	-	64	47	-	88.0	107.4
	Spray coating	1	-	82	67	-	97.0	135.2
		2	-	-	90	-	-	146.9
Renapur	Spin coating	1	78	53	37	47.9	78.2	88.4
		2	67	52	34	45.1	77.2	82.1
	Spray coating	1	-	-	71	-	-	138.9
		2	-	85	74	-	97.6	141.2

The force required to initiate droplet movement is computed based on the diagram in Figure 6 using the following equilibrium equation:

$$F = mg \sin \alpha \tag{3}$$

where, F is the force required to initiate droplet sliding, m is the mass of the DI water droplet, g is the gravitational acceleration (9.81 ms^{-2}) and α is the sliding angle recorded when the droplet begins to move. The mass of the water

droplet is $m = \rho V$, where ρ is the DI water density (0.997 g/mL) and V is the DI water volume. The results are analysed and presented in Table 2 and Figure 7. Surfaces that failed to initiate any movement after 90° sliding angle are not indicated in Figure 7 and the force was not calculated.

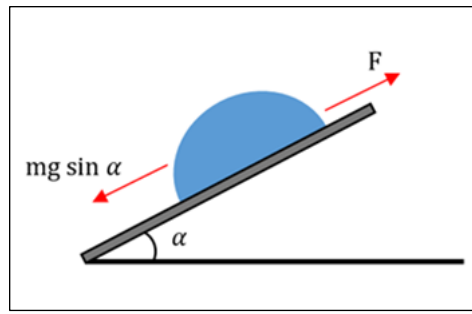

Figure 6: Droplet begins to slide on the tilted sample surface at an angle, α. The force required to initiate the movement is mg sin α

When comparing the two deposition methods (Figure 7), spin coating yielded the best results, as almost all samples were able to induce sliding for the 5 µL, 10 µL, and 15 µL droplet volumes. The 2-layer spin-coated Renapur surface demonstrates the best overall performance, requiring the least force to initiate droplet sliding at 82.1 µN. For the spray coating method, the 1-layer Liquiproof surface exhibits the lowest force required for droplet movement, measuring 97.0 µN and 135.2 µN for droplets of 10 µL and 15 µL, respectively. The subpar performance of the spray-coated samples for both Renapur and Liquiproof is postulated to be a result of their higher surface roughness compared to the spin-coated surfaces, leading to increased resistance to motion. The sliding angle increases with surface roughness for hydrophobic surfaces, but decreases significantly when the roughness reaches a certain threshold, transitioning the surface behaviour to superhydrophobic [40]-[41].

The relationship between contact angle hysteresis (CAH) and sliding angle can be expressed by Equation (4) [38]-[39]:

$$\frac{mg \sin \alpha}{w} = \gamma_{lg}(\cos \theta_R - \cos \theta_A) \quad (4)$$

where w is the width of the droplet. From Equation (4), it is evident that a droplet can move easily with a low sliding angle when the CAH is very small [42]. Figure 8 depicts a plot of sin α against $\cos \theta_R - \cos \theta_A$, where the slope represents the constant $\gamma_{lg} w/mg$. Each of the eight data points represents the CAH and sliding angle measurements of the eight surfaces for the 15 µL droplet. As observed from the plot, the experimental data approximately

conforms to Equation (4), indicating that the sliding angle and the resistance force to droplet motion increase linearly with CAH. The dashed blue line represents the linear regression fit for the data.

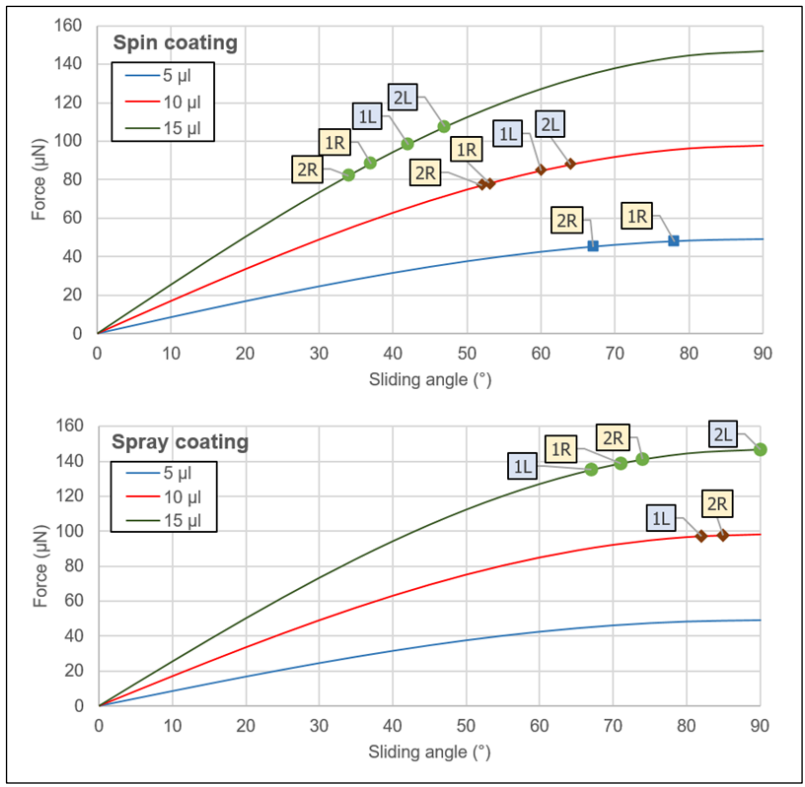

Figure 7: Force required for droplet sliding down on the Liquiproof and Renapur hydrophobic surfaces prepared using different deposition methods with different numbers of layers. 1R, 2R, 1L, 2L represent 1-layer Renapur, 2-layer Renapur, 1-layer Liquiproof, and 2-layer Liquiproof respectively

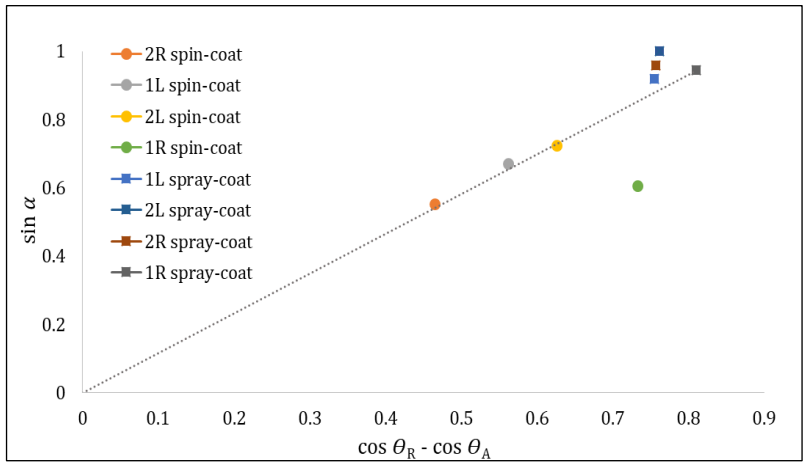

Figure 8: Sliding angle, α of 15 µL droplet as a function advancing and receding angles on the eight hydrophobic surfaces. Each data point represents each of the sample types. The dashed line is the linear fit to the experimental data.

Conclusions

In this study, two hydrophobic materials were investigated, with the Renapur material showing particularly promising surface performance, especially when applied using the spin coating deposition method. The best-performing sample, a 2-layer spin-coated Renapur, recorded the lowest contact angle hysteresis at 28° and the lowest sliding angle at 34°, which corresponds to a force of 82.1 µN required to move the droplet contact line.

For comparison, the benchmark hydrophobic material for electrowetting applications, Cytop®, has a sliding angle of 27° - 30° and a CAH ranging between 3° - 12° depending on the film thickness [43]. We hypothesise that the hydrophobic material Renapur, proposed by this study can be further improved to achieve performance as good as or better than Cytop® and Teflon™ AF by increasing the film thickness of the spin-coated surface, as indicated by the results obtained so far.

Low-cost materials with easy deposition methods can pave the way for wider adoption of electrowetting-on-dielectric (EWOD) technology, specifically for single-use disposable chips used in point-of-care diagnostics during disasters or in remote areas. The results from this study demonstrate that commercial hydrophobic materials have the potential to be utilised as the actuating surface in the future development of EWOD devices.

Contributions of Authors

The authors confirm the equal contribution in each part of this work. All authors reviewed and approved the final version of this work.

Funding

This work was supported by the "Geran Penyelidikan Lestari 600-RMC/MYRA 5/3/LESTARI (010/2020)" from Universiti Teknologi MARA, Malaysia.

Conflict of Interests

All authors declare that they have no conflicts of interest.

Acknowledgment

The authors are grateful to receive Geran Penyelidikan Lestari 600-RMC/MYRA 5/3/LESTARI (010/2020) from Universiti Teknologi MARA, Malaysia which help to fund this research project. We are also grateful for the support provided by College of Engineering, UiTM Shah Alam.

References

[1] M. Z. Khan, J. Militky, M. Petru, B. Tomková, A. Ali, E. Tören, S. Perveen, "Recent advances in superhydrophobic surfaces for practical applications: A review," *European Polymer Journal*, vol. 178, no. 2, pp. 1-10, 2022.

[2] C. Yang, U. Tartaglino, and B. N. J. Persson, "Influence of surface roughness on superhydrophobicity", *Physical Review Letters*, vol. 97, no. 11, pp. 1-4, 2006.

[3] H. Chen, H. Fan, N. Su, R. Hong, and X. Lu, "Highly hydrophobic polyaniline nanoparticles for anti-corrosion epoxy coatings," *Chemical Engineering Journal*, vol. 420, pp. 1-10, 2021.

[4] A. O. Ijaola, P. K. Farayibi, and E. Asmatulu, "Superhydrophobic coatings for steel pipeline protection in oil and gas industries: A comprehensive review," *Journal of Natural Gas Science and Engineering*, vol. 83, pp. 1-24, 2020.

[5] S. Brown, J. Lengaigne, N. Sharifi, M. Pugh, C. Moreau, A. Dolatabadi,

L. Martinu, and J. E. Klemberg-Sapieha, "Durability of superhydrophobic duplex coating systems for aerospace applications", *Surface and Coatings Technology*, vol. 401, pp. 1-12, 2020.

[6] C. Desrousseaux, V. Sautou, S. Descamps, and O. Traoré, "Modification of the surfaces of medical devices to prevent microbial adhesion and biofilm formation," *Journal of Hospital Infection*, vol. 85, no. 2, pp. 87–93, 2013.

[7] D. Ahmad, I. Van Den Boogaert, J. Miller, R. Presswell, and H. Jouhara, "Hydrophilic and hydrophobic materials and their applications", *Energy Sources, Part A: Recovery, Utilization, and Environment Effects*, vol. 40, no. 22, pp. 2686–2725, 2018.

[8] M. K. Mehrizi and Z. Shahi, "A Review on Hydrophobicity and Fabricating Hydrophobic Surfaces on the Textiles" in *Sustainable Practices in the Textile Industry*, Springer, 2021, pp. 149–165.

[9] H. Jiang, R. Qian, T. Yang, Y. Guo, D. Yuan, B. Tang, R. Zhou, H. Li, G. Zhou, "Inkjet-printed dielectric layer for the enhancement of electrowetting display devices", *Nanomaterials*, vol. 14, no. 4, 2024. doi: 10.3390/nano14040347

[10] M. G. Pollack, R. B. Fair, and A. D. Shenderov, "Electrowetting-based actuation of liquid droplets for microfluidic applications", *Applied Physics Letters*, vol. 77, no. 11, pp. 1725–1726, 2000. doi: 10.1063/1.1308534

[11] F. Mugele and J. Heikenfeld, Electrowetting: Fundamental Principles and Practical Applications, John Wiley & Sons, 2018.

[12] L. Meng, M. Li, Z. Xu, A. Lv, Y. Jia, M. Chen, P. I. Mak, R. P. Martins, M.K. Law, "Absolute quantification of nucleic acid on digital microfluidics platform based on superhydrophobic–superhydrophilic micropatterning", *Sensors Actuators B: Chemical*, vol. 402, pp. 1-10, 2024. doi: 10.1016/j.snb.2023.135079

[13] J. Li, "Current commercialization status of electrowetting-on-dielectric (EWOD) digital microfluidics", *Lab on a Chip*, vol. 20, no. 10, pp. 1705–1712, 2020.

[14] Q. Ruan, F. Zou, Y. Wang, Y. Zhang, X. Xu, X. Lin, T. Tian, H. Zhang, L. Zhou, Z. Zhu, C. Yang, "Sensitive, rapid, and automated detection of DNA methylation based on digital microfluidics", *ACS Applied Materials & Interfaces*, vol. 13, no. 7, pp. 8042–8048, 2021.

[15] S. C. C. Shih, P. C. Gach, J. Sustarich, B. A. Simmons, P. D. Adams, S. Singh, A. K. Singh, "A droplet-to-digital (D2D) microfluidic device for single cell assays", *Lab on a Chip*, vol. 15, no. 1, pp. 225–236, 2015.

[16] J. Zhai, H. Li, A. H. H. Wong, C. Dong, S. Yi, Y. Jia, P. I. Mak, C. X. Deng, R. P. Martins, "A digital microfluidic system with 3D microstructures for single-cell culture", *Microsystems & Nanoengineering*, vol. 6, no. 1, pp. 1–10, 2020. doi: 10.1038/s41378-019-0109-7

[17] L. Coudron, M. B. McDonnell, I. Munro, D. K. McCluskey, I. D. Johnston, C. K. L. Tan, M. C. Tracey, "Fully integrated digital microfluidics platform for automated immunoassay; a versatile tool for rapid, specific detection of a wide range of pathogens", *Biosensors & Bioelectronics*, vol. 128, pp. 52-60, 2018.

[18] V. D. Trung, P. A. Le, J. Natsuki, W. Zhao, T. V. B. Phung, and T. Natsuki, "Recent developments in droplet-based devices", *Materials Today Chemistry*, vol. 36, pp. 1-25, 2024. doi: 10.1016/j.mtchem.2024.101943

[19] T. G. Foat, W. J. Sellors, M. D. Walker, P. A. Rachwal, J. W. Jones, D. D. Despeyroux, L. Coudron, I. Munro, D. K. McCluskey, C. K. Tan, M. C. Tracey, "A prototype personal aerosol sampler based on electrostatic precipitation and electrowetting-on-dielectric actuation of droplets," *Journal of Aerosol Science*, vol. 95, pp. 43–53, 2016.

[20] M. Jönsson-Niedziółka, F. Lapierre, Y. Coffinier, S. J. Parry, F. Zoueshtiagh, T. Foat, V. Thomy, R. Boukherroub, "EWOD driven cleaning of bioparticles on hydrophobic and superhydrophobic surfaces", *Lab on a Chip*, vol. 11, no. 3, pp. 490–496, 2011.

[21] J. B. Chae, J. O. Kwon, J. S. Yang, D. Kim, K. Rhee, and S. K. Chung, "Optimum thickness of hydrophobic layer for operating voltage reduction in EWOD systems", *Sensors Actuators A: Physical*, vol. 215, pp. 8–16, 2014.

[22] E. N. A. Latip, L. Coudron, M. B. McDonnell, I. D. Johnston, D. K. McCluskey, R. Day, M. C. Tracey, "Protein droplet actuation on superhydrophobic surfaces: A new approach toward anti-biofouling electrowetting systems", *RSC Advances*, vol. 7, no. 78, pp. 49633-49648, 2017. doi: 10.1039/c7ra10920b

[23] X. Xu, L. Cai, S. Liang, Q. Zhang, S. Lin, M. Li, Q. Yang, C Li, Z Han, C. Yang, "Digital microfluidics for biological analysis and applications", *Lab on a Chip*, vol. 23, no. 5, pp. 1169–1191, 2023.

[24] A. H. C. Ng, R. Fobel, C. Fobel, J. Lamanna, D. G. Rackus, A. Summers, C. Dixon, M. D. M. Dryden, C. Lam, M. Ho, N. S. Mufti, "A digital microfluidic system for serological immunoassays in remote settings", *Science Translational Medicine*, vol. 10, no. 438, pp. 1-12, 2018.

[25] S. Smith, M. Sypabekova, and S. Kim, "Double-sided tape in microfluidics: A cost-effective method in device fabrication", *Biosensors*, vol. 14, no. 5, pp. 1-28, 2024. doi: 10.3390/bios14050249

[26] K. Leirs, F. Dal Dosso, E. Perez-Ruiz, D. Decrop, R.Cops, J.Huff, M. Hayden, N. Collier, K. X. Yu, S. Brown, J. Lammertyn, "Bridging the gap between digital assays and point-of-care testing: Automated, low cost, and ultrasensitive detection of thyroid stimulating hormone", *Analytical Chemistry*, vol. 94, no. 25, pp. 8919-8927, 2022.

[27] V. Soum, Y. Kim, S. Park, M. Chuong, S. R. Ryu, S. H. Lee, G. Tanev, J. Madsen, O. S. Kwon, K. Shin, "Affordable fabrication of conductive

electrodes and dielectric films for a paper-based digital microfluidic chip", *Micromachines*, vol. 10, no. 2, p. 109, 2019.

[28] V. Narasimhan and S.-Y. Park, "An ion gel as a low-cost, spin-coatable, high-capacitance dielectric for electrowetting-on-dielectric (EWOD)", *Langmuir*, vol. 31, no. 30, pp. 8512–8518, 2015.

[29] Y. Li, R. Chen, and R. J. Baker, "A fast fabricating electro-wetting platform to implement large droplet manipulation," *2014 IEEE 57th International Midwest Symposium on Circuits and Systems*, pp. 326–329, 2014.

[30] J. Cai, J. Jiang, J. Jiang, Y. Tao, X. Gao, M. Ding, Y. Fan, "Fabrication of transparent and flexible digital microfluidics devices", *Micromachines*, vol. 13, no. 4, pp. 1-9, 2022.

[31] M. Abdelgawad and A. R. Wheeler, "Low-cost, rapid-prototyping of digital microfluidics devices", *Microfluidics and Nanofluidics*, vol. 4, no. 4, pp. 349-355, 2008.

[32] M. Yafia, S. Shukla, and H. Najjaran, "Fabrication of digital microfluidic devices on flexible paper-based and rigid substrates via screen printing," *Journal of Micromechanics Microengineering*, vol. 25, no. 5, pp. 1-11, 2015.

[33] A. Abadian and S. Jafarabadi-Ashtiani, "Paper-based digital microfluidics", *Microfluidics and Nanofluidics*, vol. 16, no. 5, pp. 989–995, 2014.

[34] B. Parsi, J. Augenstein, R. D. Maynes, and N. B. Crane, "A low-cost electrowetting on dielectric semi-continuous pump for application to microfluidic reconfigurable devices", *Experimental Thermal and Fluid Science*, vol. 155, pp. 1-14, 2024. doi: 10.1016/j.expthermflusci.2024.111183

[35] T. Huhtamäki, X. Tian, J. T. Korhonen, and R. H. A. Ras, "Surface-wetting characterization using contact-angle measurements", *Nature Protocol*, vol. 13, no. 7, pp. 1521–1538, 2018.

[36] S. Azizian and M. Khosravi, "Advanced oil spill decontamination techniques," in *Interface Science and Technology*, vol. 30, Elsevier, 2019, pp. 283–332.

[37] S. Suzuki, A. Nakajima, M. Sakai, Y. Sakurada, N. Yoshida, A. Hashimoto, Y. Kameshima, K. Okada, "Slipping and rolling ratio of sliding acceleration for a water droplet sliding on fluoroalkylsilane coatings of different roughness", *Chemistry Letters*, vol. 37, no. 1, pp. 58–59, 2008.

[38] H. J. Butt, J. Liu, K. Koynov, B. Straub, C. Hinduja, I. Roismann, R. Berger, X. Li, D. Vollmer, W. Steffen, and M. Kappl, "Contact angle hysteresis", *Current Opinion in Colloid and Interface Science*, vol. 59, pp. 1-9, 2022.

[39] K.-Y. Law, "Contact angle hysteresis on smooth/flat and rough surfaces. Interpretation, mechanism, and origin", *Accounts of Materials Research*,

vol. 3, no. 1, pp. 1–7, 2021.

[40] M. Miwa, A. Nakajima, A. Fujishima, K. Hashimoto, and T. Watanabe, "Effects of the surface roughness on sliding angles of water droplets on superhydrophobic surfaces", *Langmuir*, vol. 16, no. 13, pp. 5754–5760, 2000.

[41] J. J. Bikerman, "Sliding of drops from surfaces of different roughnesses," *Journal of Colloid Science*, vol. 5, no. 4, pp. 349–359, 1950.

[42] S. Y. Chen, Y. Kaufman, A. M. Schrader, D. Seo, D. W. Lee, S.H. Page, P. H. Koenig, S. Isaacs, Y.Gizaw, J.N.Israelachvili, "Contact angle and adhesion dynamics and hysteresis on molecularly smooth chemically homogeneous surfaces", *Langmuir*, vol. 33, no. 38, pp. 10041–10050, 2017.

[43] J. B. Chae, J. O. Kwon, J. S. Yang, K. Rhee, and S. K. Chung, "Investigation on the thickness effect of a hydrophobic layer for operating voltage reduction in EWOD systems," *IEEE 26th International Conference on Micro Electro Mechanical Systems*, vol. 19, pp. 1109–1112, 2013.